Molecular Therapy
Nucleic Acids
Original Article

The SWIB/MDM2 motif of UBE4B activates the p53 pathway

H. Helena Wu,[1] Sarah Leng,[2] Yasser Abuetabh,[1] Consolato Sergi,[2,3] David D. Eisenstat,[4,5,6,7] and Roger Leng[1]

[1]370 Heritage Medical Research Center, Department of Laboratory Medicine and Pathology, University of Alberta, Edmonton, AB T6G 2S2, Canada; [2]Department of Laboratory Medicine and Pathology (5B4. 09), University of Alberta, Edmonton, AB T6G 2B7, Canada; [3]Division of Anatomical Pathology, Children's Hospital of Eastern Ontario (CHEO), University of Ottawa, 401 Smyth Road, Ottawa, ON K1H 8L1, Canada; [4]Department of Oncology, Cross Cancer Institute, 11560 University Avenue, University of Alberta, Edmonton, AB T6G 1Z2, Canada; [5]Department of Pediatrics, University of Alberta, 11405 - 87 Avenue, Edmonton, AB T6G 1C9, Canada; [6]Department of Medical Genetics, University of Alberta, 8613 114 Street, Edmonton, AB T6G 2H7, Canada; [7]Murdoch Children's Research Institute, Department of Paediatrics, University of Melbourne, 50 Flemington Road, Parkville, VIC 3052, Australia

The tumor suppressor p53 plays a critical role in cancer pathogenesis, and regulation of p53 expression is essential for maintaining normal cell growth. UBE4B is an E3/E4 ubiquitin ligase involved in a negative-feedback loop with p53. UBE4B is required for Hdm2-mediated p53 polyubiquitination and degradation. Thus, targeting the p53-UBE4B interactions is a promising anticancer strategy for cancer therapy. In this study, we confirm that while the UBE4B U box does not bind to p53, it is essential for the degradation of p53 and acts in a dominant-negative manner, thereby stabilizing p53. C-terminal UBE4B mutants lose their ability to degrade p53. Notably, we identified one SWIB/Hdm2 motif of UBE4B that is vital for p53 binding. Furthermore, the novel UBE4B peptide activates p53 functions, including p53-dependent transactivation and growth inhibition, by blocking the p53-UBE4B interactions. Our findings indicate that targeting the p53-UBE4B interaction presents a novel approach for p53 activation therapy in cancer.

INTRODUCTION

The tumor suppressor p53 is critical for preventing tumor development.[1–5] Genetic and clinical studies have shown the importance of p53 in safeguarding genomes. p53-Deficient mice are highly tumor susceptible, and more than 75% of $p53^{-/-}$ mice develop tumors in 6 months.[1] p53 is inactivated in more than 50% of all human tumors.[1–5] This suggests that loss of p53 plays a vital role in the pathogenesis of cancer and that regulation of p53 expression and stability is essential for maintaining normal cell growth. Mdm2 (called Hdm2 or MDM2 in humans) binds to the p53 transactivation domain and promotes p53 degradation via a ubiquitin-proteasome pathway.[6–11] The deletion of Mdm2 in the mouse results in a lethal embryonic phenotype.[12,13] However, this early embryonic death of Mdm2-null mice is rescued by further depleting the *p53* gene, thus indicating the importance of the negative regulatory function of Hdm2 on p53 during development.[12,13] Moreover, the Hdm2 gene itself is transcriptionally activated by p53,[14] forming an autoregulatory feedback loop that restrains p53 activity.[14–16]

The proteasome efficiently recognizes polyubiquitin chains.[17–19] It has been demonstrated that Mdm2 mediates monoubiquitination or multiple ubiquitination of p53.[20–23] These results were further confirmed using methylated ubiquitin (Ub) as a control.[20] Mdm2 does not polyubiquitinate p53 *in vitro*, which suggests that the activity of other Ub ligases is required for Mdm2-mediated p53 polyubiquitination and degradation.[20–23]

Human UBE4B is a mammalian homolog of the protein Ufd2 found in *S. cerevisiae*.[24,25] Yeast Ufd2 was the first known E4 ubiquitination factor.[26] Single Ufd2 homologs have been found in *S. cerevisiae*, *C. elegans*, *D. discoideum*, and *A. thaliana*.[27–29] Two genes related to Ufd2 have been found in *M. musculus* (named Ube4a and Ube4b or Ufd2a) and *H. sapiens* (named UBE4A and UBE4B).[26–28] NOSA, the Ufd2 homolog from *D. discoideum*, is essential for cellular differentiation.[27] Deleting Ube4b in mice results in embryonic lethality due to marked apoptosis.[29] However, the underlying mechanisms for this lethality remain unclear. The E3/E4 ligase UBE4B has several known targets for ubiquitination and degradation, including ataxin-3,[30] FEZ1,[31] p73,[32] EGFR,[33] and p53.[34] UBE4B is a critical negative regulator of p53.[34] The negative control of p53 by UBE4B has been further confirmed.[35,36] UBE4B expression is aberrantly upregulated in human brain tumors,[34] breast cancer,[37] hepatocellular tumors,[38] and nasopharyngeal carcinoma.[39]

Blocking the p53-UBE4B interaction is an attractive strategy for cancer therapy. However, the interaction between p53 and UBE4B needs to be better characterized. Here, we characterize a series of UBE4B mutants for their ability to interact with and degrade p53. We observed that C-terminal UBE4B mutants lost their ability to degrade p53. We further confirmed that the U box of UBE4B is essential for the degradation of p53. Notably, an SWIB/Hdm2 motif was identified in UBE4B. This UBE4B motif blocks the p53-UBE4B interaction and activates p53 functions, including p53-dependent transactivation and

Received 14 September 2022; accepted 1 February 2023;
https://doi.org/10.1016/j.omtn.2023.02.002.

Correspondence: Roger Leng, 370 Heritage Medical Research Center, Department of Laboratory Medicine and Pathology, University of Alberta, Edmonton, AB T6G 2S2, Canada.
E-mail: rleng@ualberta.ca

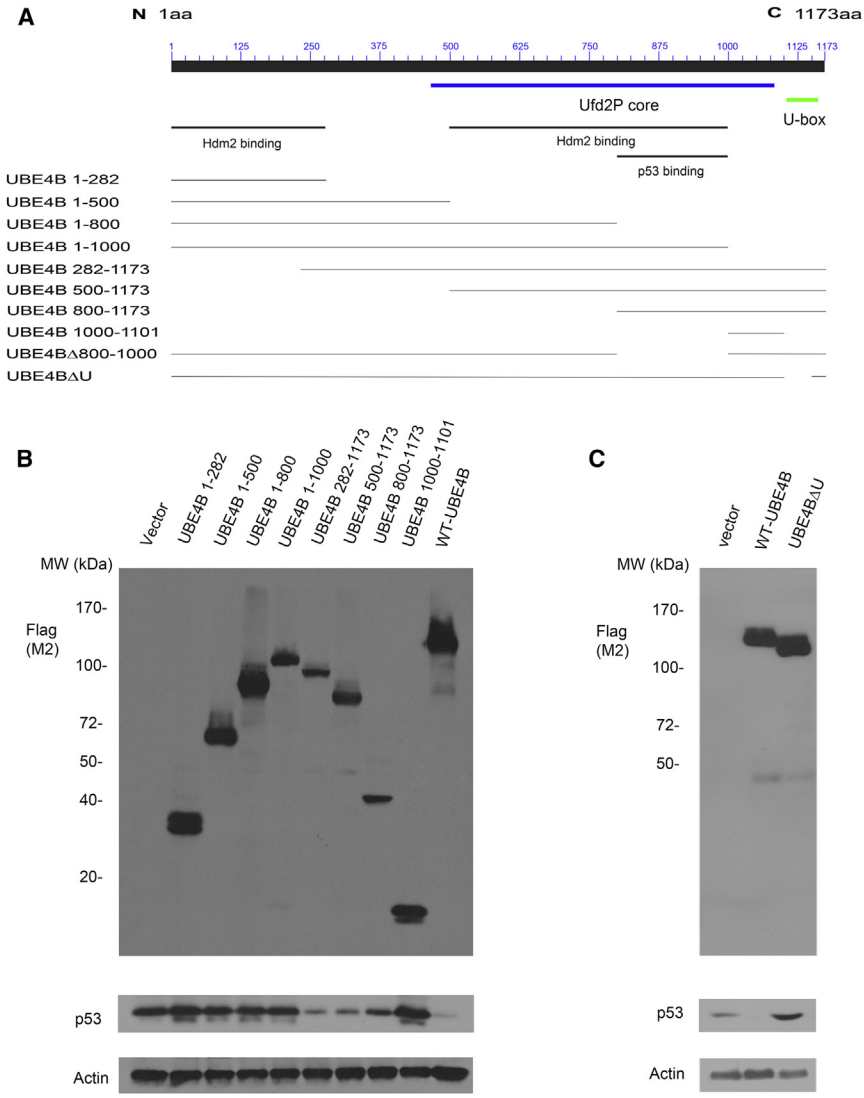

Figure 1. Analysis of a series of UBE4B truncations

(A) Schematic representation of UBE4B truncations fused to the FLAG-tagged expression vector. (B) HCT116 cells were transfected with a series of FLAG-UBE4B mutants as indicated. Cells were lysed and analyzed by immunoblotting with anti-p53 and anti-FLAG for UBE4B or various mutants of UBE4B. An antibody against β-actin was used as a loading control. (C) HCT116 cells were transfected with plasmids expressing UBE4B and UBE4BΔU as indicated. The levels of endogenous p53 were analyzed by western blotting.

growth suppression. The newly identified UBE4B peptide may provide a new approach to cancer therapy.

RESULTS

Contribution of the C terminus of UBE4B to degradation of p53 in cells

Our previous study demonstrated that UBEB4 is required for Hdm2-mediated p53 polyubiquitination and degradation.[34] Hdm2-interacting domains were mapped to two regions of UBE4B (amino acids [aa] 1–282 and 500–800). p53 was bound to the UBE4B 801–1,000 aa.[34] In this study, we sought to determine the contribution of the COOH terminus of UBE4B, which is necessary for its Ub ligase activity to p53. The UBE4B constructs were designed and generated (Figure 1A). HCT116 cells were transfected with plasmids expressing wild-type (WT) FLAG-UBE4B and various FLAG-UBE4B mutants. As shown in Figure 1B, several C-terminal mutants of UBE4B without a U box (1–282, 1–500, 1–800, 1–1,000, 1,000–1,101) lost their ability to degrade p53 compared with the cells transfected with WT-UBE4B, suggesting that the U-box domain of UBE4B is essential for its ligase function of p53. Although several N-terminal UBE4B mutants (282–1,173, 500–1,173, 800–1,173) degrade p53, the UBE4B mutant (282–1,173) significantly decreased p53 protein levels compared with the UBE4B 800–1,173 mutant, indicating that the Ufd2p core regions of UBE4B are also required for UBE4B to efficiently ubiquitinate and degrade p53. As expected, UBE4BΔU (deleted U box of UBE4B) did not target the degradation of p53, confirming that the U box of UBE4B is essential for its E3 function (Figure 1C). Notably, the UBE4BΔU stabilized the endogenous p53 protein. Taken together, our results indicated that the U-box domain and the Ufd2p core regions of UBE4B are required for degradation of p53 in cells.

Characterization of UBE4B mutants

We previously showed that residues 800–1,000 of UBE4B are required to bind p53.[34] We next generated several HCT116 stable clones expressing UBE4B and various UBE4B mutants. Endogenous levels of p53 protein decreased significantly in stable clones expressing WT-UBE4B. As expected, UBE4BΔ800–1,000 (deletion of the p53-binding domain of UBE4B) and UBE4B 1–1,000 (deletion of the U box of UBE4B) failed to degrade p53. p53 protein levels were significantly increased in HCT116 clones expressing UBE4BΔU (Figure 2A). To determine whether these UBE4B mutants are associated with p53, co-immunoprecipitation (co-IP) assays were performed. HCT116 cells were transfected with plasmids expressing FLAG-UBE4B, FLAG-UBE4BΔU, FLAG-UBE4B 500–1,173 (containing p53-binding regions), and two C-terminal truncations of FLAG-UBE4B (1–228 and 1–500) as indicated. Cell extracts were immunoprecipitated with an anti-FLAG-specific antibody (M5) and analyzed by immunoblotting. As shown in Figure 2B, p53 protein levels were significantly reduced in cells co-expressing p53 with UBE4B or UBE4B 500–1,173. However, the interaction between UBE4B and

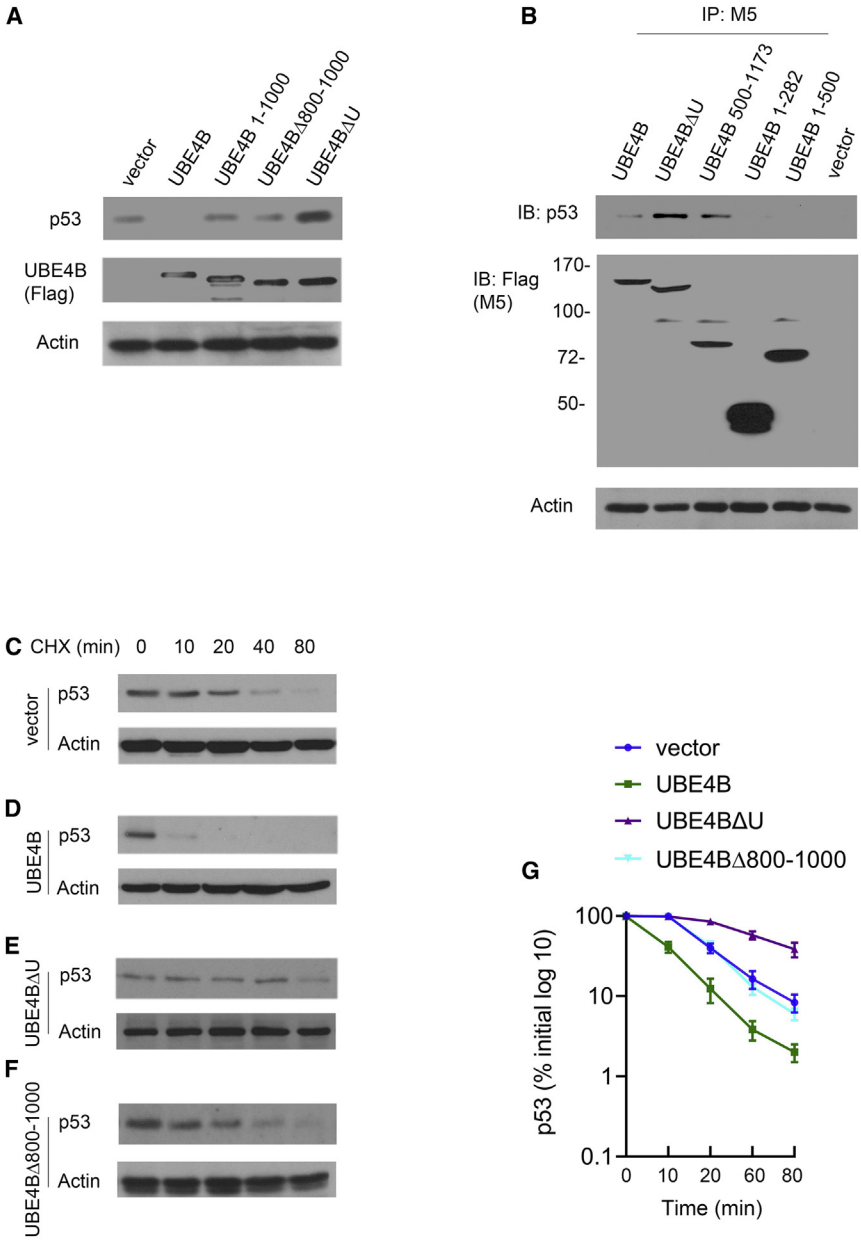

Figure 2. Stabilization of endogenous p53 by UBE4BΔU

(A) HCT116 clones stably expressing an empty vector, UBE4B, UBE4B 1–1,000, UBE4BΔ800–1,000, and UBE4BΔU were subjected to immunoblotting with indicated antibodies. An antibody against β-actin was used as a loading control. (B) HCT116 cells were transfected with plasmids expressing UBE4B and several UBE4B mutants as indicated. Cell extracts were immunoprecipitated with an anti-FLAG-specific antibody (M5) and analyzed by immunoblotting with antibodies against p53 or FLAG (M5). (C) HCT116 cells were transiently transfected with an empty vector; 24 h later, the cells were treated with cycloheximide (CHX, 20 μg/mL) for 6 h. The levels of p53 were determined by immunoblotting with a p53-specific antibody (DO-1). An antibody against β-actin was used as a loading control. (D) Similar to (C), except that HCT116 cells were transfected with the UBE4B expression plasmid. (E) Similar to (C), except that HCT116 cells were transfected with a plasmid expressing UBE4BΔU. (F) Similar to (C), except that HCT116 cells were transfected with a plasmid expressing UBE4BΔ800–1,000. (G) Expression levels of p53 in HCT116 cells were determined by immunoblot densitometry in (C), (D), (E), and (F). Error bars indicate SEM (n = 3).

p53 increased in cells transfected with a plasmid expressing UBE4BΔU, indicating that: (1) WT-UBE4B is a critical negative regulator of p53; (2) the residues 800–1,000 of UBE4B are required for p53 binding; and (3) the deleted U box of UBE4B retains the ability to bind p53 but loses its E3 activity to degrade p53. As expected, C-terminal mutants of UBE4B (1–288, 1–500) failed to bind to p53.

To further determine whether UBE4B mutants regulate p53 stability, HCT116 stable clones expressing an empty vector, UBE4B, UBE4BΔU, and UBE4BΔ800-1,000, were treated with cycloheximide (CHX) to inhibit *de novo* protein synthesis. We observed that the half-life of endogenous p53 was approximately 10 min in the presence of UBE4B compared with the clones expressing an empty vector (approximately 30 min) (Figures 2C and 2D). In contrast, the half-life of p53 was increased to approximately 60 min in the presence of UBE4BΔU and remained approximately 30 min in the presence of UBE4BΔ800–1,000 (Figures 2E and 2F). The levels of p53 protein were determined by densitometry and plotted (Figure 2G). Our findings demonstrated that residues 800–1,000 of UBE4B are the key to the p53-UBE4B interaction.

The U box of UBE4B is essential for ubiquitination of p53 in cells and *in vitro*

Next, we investigated whether UBE4B-mediated p53 ubiquitination is influenced by UBE4B truncations in cells. Plasmids expressing p53 or in combination with various mutants of UBE4B were transfected into HCT116, $p53^{-/-}$ cells. Cells were harvested, immunoprecipitated with a p53-specific antibody, and analyzed by western blotting. To avoid protein that co-immunoprecipitated with p53, co-IP was performed under denatured conditions using RIPA buffer with SDS.[34,40] The p53 immunoblot revealed that p53 was highly ubiquitinated in the presence of WT-UBE4B, UBE4B 282–1,173, and UBE4B 500–1,173 compared with C-terminal mutants of UBE4B (1–282, 1–500, 1–800) (Figure 3A, top panel). The expression of various UBE4B mutants was measured by immunoblotting (Figure 3A, bottom panel). To determine whether UBE4BΔ800–1,000 has intrinsic Ub ligase

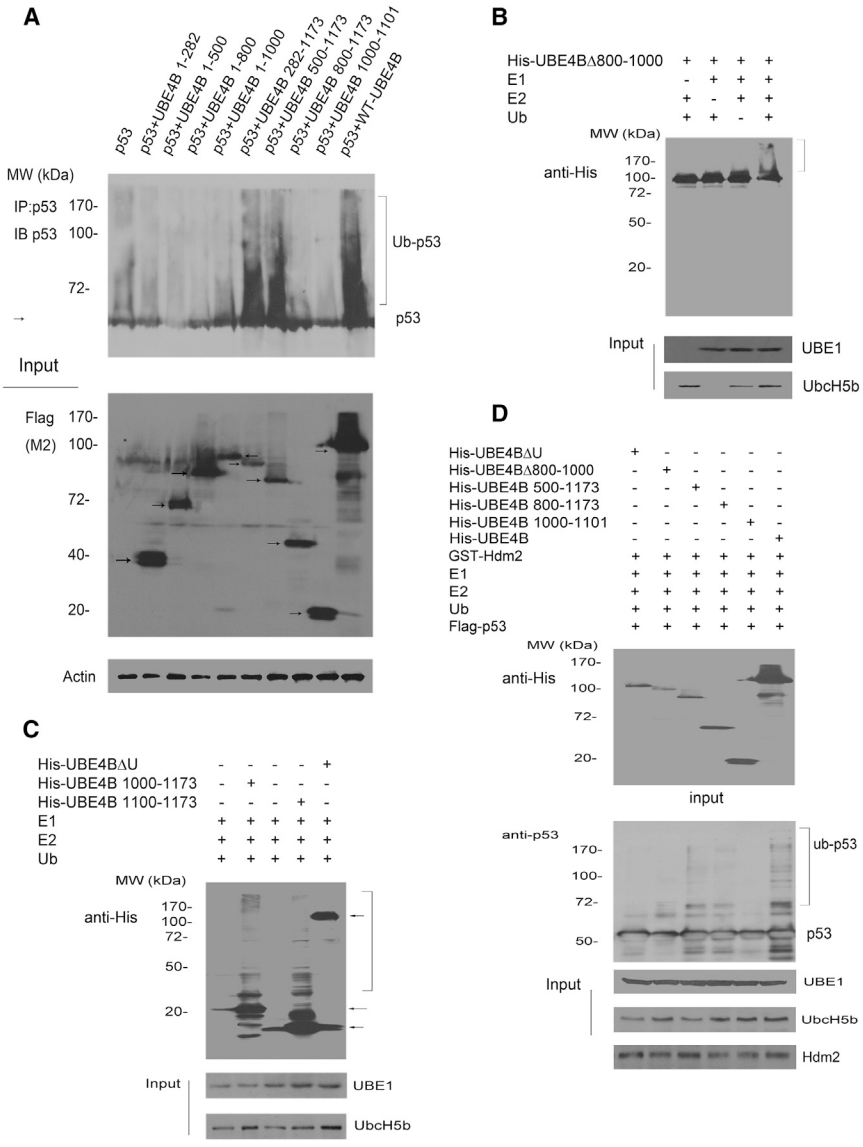

Figure 3. The C-terminal truncations of UBE4B contribute to its ligase activity to p53

(A) HCT116, p53$^{-/-}$ cells were transfected with plasmids expressing p53 or co-expression of various UBE4B constructs as indicated. Cells were lysed using RIPA buffer with SDS, immunoprecipitated with a specific antibody for p53 (Pab1801), and analyzed by immunoblotting with antibodies against p53 (upper panel, DO-1) or anti-FLAG for UBE4B constructs (lower panel, M2). β-Actin was used as a loading control. The arrow indicates the position of UBE4B mutants. (B) His-UBE4BΔ800–1,000 was evaluated for its self-ubiquitination activity in the presence of recombinant E1 (UBE1), E2 (UbcH5b), and ubiquitin (Ub) as indicated. Following the ubiquitination reaction, the samples were subjected to SDS-PAGE and immunoblotting with a His antibody to reveal ubiquitinated products. (C) His-UBE4BΔU, His-UBE4B 1,000–1,173, and His-UBE4B 1,100–1,173 fusion proteins were purified from *E. coli* and evaluated for their ligase activity in the presence of E1, E2, and Ub, as indicated. The self-ubiquitination of UBE4B mutants was detected by immunoblotting with an anti-His antibody to reveal ubiquitinated products. (D) His-UBE4B and various truncated His-UBE4B fusion proteins were affinity purified from *E. coli* and analyzed by western blotting with an anti-His antibody (top image, input). Various His-UBE4B constructs were evaluated for their ability to ubiquitinate purified p53 protein in the presence of GST-Hdm2 and analyzed by immunoblotting with a p53-specific antibody (DO-1) to detect ubiquitinated p53 (middle image). Purified E1 (UBE1), E2 (UbcH5b), and GST-Hdm2 are shown in the bottom three lanes.

activity, an *in vitro* ubiquitination assay was performed.[34,40] The UBE4BΔ800–1,000 mediated self-ubiquitination was readily detected and depended on the presence of E1, E2, and Ub (Figure 3B, top panel). We then evaluated UBE4B self-ubiquitination in the presence or absence of the U-box domain of UBE4B *in vitro*. As shown in Figure 3C, UBE4BΔU lost its self-ubiquitination compared with UBE4B 1,000–1,173 and UBE4B 1,100–1,173, confirming that the U box of UBE4B is essential for its ubiquitination activity *in vitro*. We further investigated whether UBE4B variants could ubiquitinate p53 *in vitro*. His-UBE4B and various truncated His-UBE4B fusion proteins were affinity purified from *E. coli* and analyzed by immunoblotting (Figure 3D, top image). His-UBE4B or various truncated His-UBE4B fusion proteins were then incubated with purified FLAG-p53, and glutathione S-transferase (GST)-Hdm2 fusion proteins in the presence of E1, E2, and Ub.[34,41,40] The p53 immunoblot revealed that multiple ubiquitinated or polyubiquitinated p53 occurred to a lesser extent with UBE4B 500–1,173 and UBE4B 800–1,173 than with WT-UBE4B in the presence of E1, E2, Ub, and Hdm2 (Figure 3D, middle image). In addition, these data indicated that both mutants (UBE4B 500–1,173 and UBE4B 800–1,173, which have a partial deletion of the Ufd2 core [462–1,082 aa]) retain their ubiquitination activity. UBE4BΔU and UBE4B 1,000–1,101 lost their role in p53 ubiquitination. Notably, UBE4BΔ800–1,000 (unable to bind to p53 with the U box) failed to mediate p53 polyubiquitination, implying that the p53-UBE4B interaction is required for UBE4B-mediated ubiquitination of p53. The levels of UBE1, UbcH5b, and GST-Hdm2 proteins were detected by western blotting (Figure 3D, bottom panels). Together, our results demonstrated that the UBE4B U-box domain is essential for UBE4B-mediated ubiquitination of p53 in cells and *in vitro*.

Characterization of the functional consequences of UBE4B mutants that interact with p53

To determine the functional consequences of UBE4B mutants that interact with p53, we investigated the effect of UBE4B mutant expression on p53-mediated transcriptional activation. Plasmids expressing

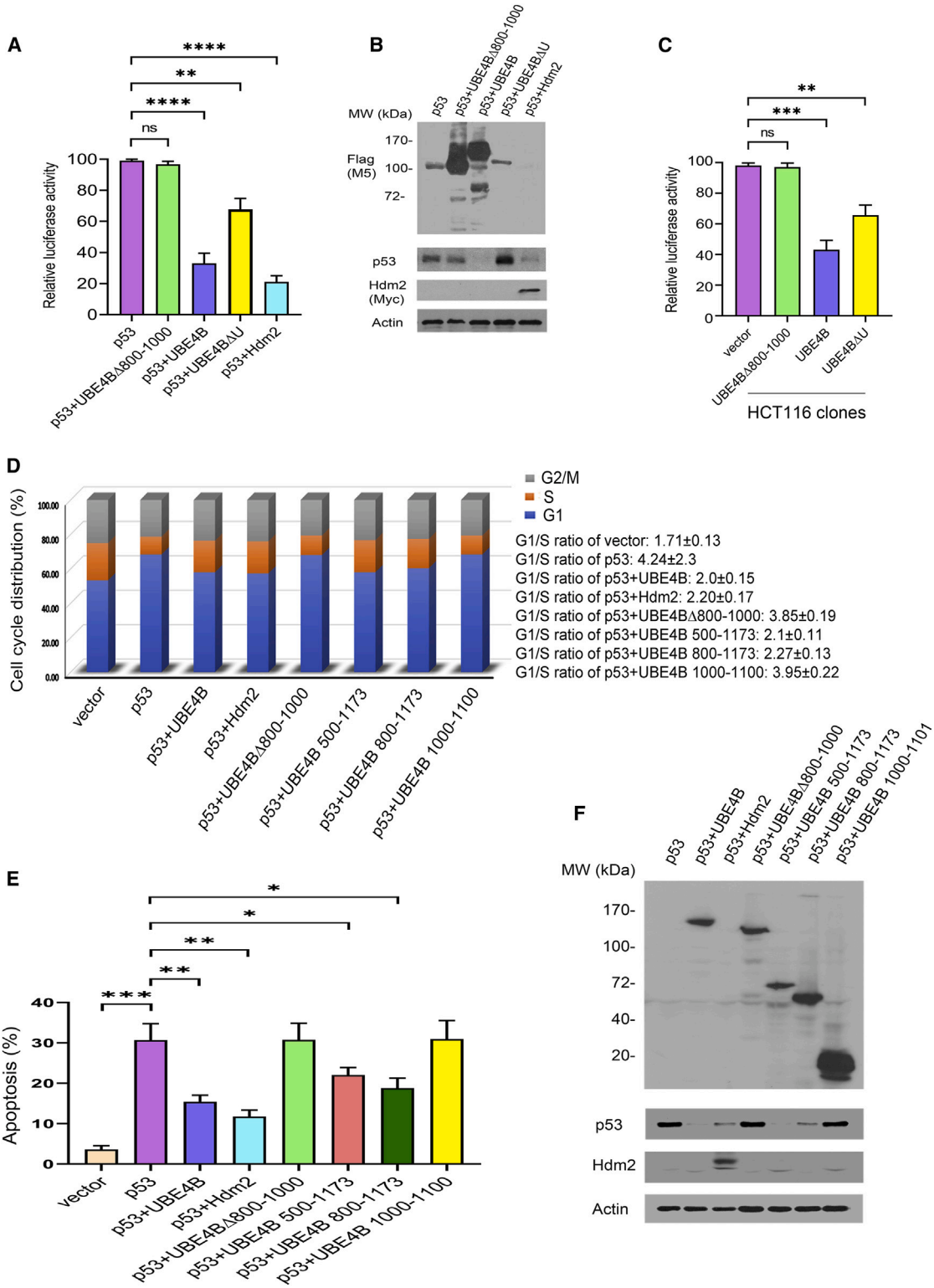

Figure 4. Effect of various UBE4B mutants on p53 functions

(A) HCT116, p53$^{-/-}$ cells were co-transfected with a reporter plasmid for p21-luciferase (Luc), and a p53 expression construct in combination with UBE4BΔ800–1,000, UBE4B, UBE4BΔU, or Hdm2 expression constructs, or an empty vector. Transcriptional activity of p53 is shown; error bars indicate SEM (n = 3). **p < 0.01; ****p < 0.0001.

(legend continued on next page)

a p21-Luc reporter, p53, in combination with UBE4B or UBE4B mutants or Hdm2 were transfected into HCT116, $p53^{-/-}$ cells.[34,41] UBE4B and Hdm2 both repressed p53-mediated transcriptional activity, and UBE4BΔU retained its ability to repress p53 transactivation (Figure 4A). Notably, UBE4BΔ800–1,000 lost its ability to repress p53-mediated transactivation, implying that the UBE4B-p53 interaction is required for UBE4B to inhibit p53-dependent transcriptional activity. The levels of p53 and UBE4B mutant proteins were measured by western blotting (Figure 4B). We then transfected the reporter p21-Luc into HCT116 stable clones expressing UBE4B, UBE4BΔU, and UBE4BΔ800–1,000. Luciferase activity was significantly decreased in cells expressing UBE4B and UBE4BΔU (Figure 4C). In contrast, luciferase activity did not change in cells stably expressing UBE4BΔ800–1,000. These data indicated that UBE4B represses p53-dependent transactivation and that this repression does not require the U-box domain of UBE4B. It also revealed that the p53-UBE4B interaction is necessary for UBE4B to inhibit the transactivation function of p53. p53-Mediated cell-cycle arrest or apoptosis is considered important for its tumor-suppression function. To determine whether UBE4B mutants affect p53-dependent cell-cycle arrest, HCT116, $p53^{-/-}$ cells were transfected with plasmids expressing an empty vector, p53, or with UBE4B, Hdm2, and UBE4B mutants. Cell-cycle analysis was performed using propidium iodide staining followed by flow cytometry.[34,41,40] The relative proportion of cells in each phase (G_1, S, and G_2/M) of the cell cycle was determined using FlowJo software (TreeStar). The G_1/S ratio has been used as an indicator of G_1 arrest.[34,41] p53 expression increased the proportion of cells in G_1 and decreased the proportion of cells in S phase, resulting in an increase in the G_1/S ratio from 1.7 to 4.2. The N-terminal truncations of UBE4B (500–1,173 and 800–1,173) repressed p53-mediated G_1 arrest; however, UBE4BΔ800–1,000 and UBE4B 1,000–1,100 (both are unable to bind to p53) failed to inhibit p53-induced G_1 arrest, further confirming that the interaction between UBE4B and p53 is important for UBE4B to inhibit p53-dependent cell-cycle arrest (Figure 4D). UBE4B-deletion mutants were utilized to identify the regions of UBE4B that were required to inhibit p53-dependent apoptosis. HCT116, $p53^{-/-}$ cells were transfected with an empty vector, p53 alone, or p53 in combination with UBE4B, Hdm2, or UBE4B mutants. Annexin V staining was used to determine whether the truncations of UBE4B could rescue cells from p53-dependent cell death. As shown in Figure 4E, p53 expression alone resulted in apoptosis, while apoptosis was prevented mainly by co-expression of p53 with UBE4B or with Hdm2. Consistently, the N-terminal truncations of UBE4B (500–1,173 and 800–1,173) repressed p53-induced apoptosis, while UBE4BΔ800–1,000 and UBE4B 1,000–1,100 lost their ability to prevent p53-dependent apoptosis. Western blotting was used to visualize the ectopic expression levels of p53, UBE4B, Hdm2, and various UBE4B mutants (Figure 4F).

Identification of an SWIB/Hdm2 motif of UBE4B

Since the discovery of p53 in 1979, massive efforts have been underway in numerous laboratories and pharmaceutical companies to generate p53-based anticancer therapies, such as restoring WT p53 function, identifying drugs to activate p53, targeting the Hdm2-p53 interaction using small molecules, peptides, antisense, and small interfering RNA approaches, and p53 vaccines.[42–50] Several peptides derived from the N-terminal sequences of Hdm2 and p53 were shown to activate p53-induced cell-cycle arrest and apoptosis and exhibited promise in phase I and phase II clinical trials.[46–50] Targeting the p53-UBE4B interaction may provide a promising approach for p53 directed therapy. We sought to determine the precise sequence in which UBE4B binds p53. We found a putative "SWIB" motif in UBE4B by computational analysis (The Eukaryotic Linear Motif resource for Functional Sites in Proteins, http://elm.eu.org/). The identified sequences contain a putative SWIB motif (FKSLWQNI) defined by the consensus pattern F[^P]^{1}W[^P]^1[VIL] (http://elm.eu.org/ and https://prosite.expasy.org/doc/PS51925). The SWIB motif is conserved and was originally found in BAF60b proteins.[51] The SWIB motif (an amphipathic α helix) was also found in p53 family members that bind to the hydrophobic cleft of the SWIB domain of Hdm2 (also called the SWIB/Hdm2 motif). Two SWIB motifs were found in NUMB (577–584 aa and 616–623 aa of NUMB).[52] Although NUMB inhibited Hdm2-mediated p53 ubiquitination and degradation by disrupting the p53-Hdm2 interaction, the role of the SWIB motifs of NUMB remains unknown. A previous report showed that the SWIB and Hdm2 domains are homologous and share a similar function.[51] An SWIB-like domain in Hdm2 has been identified (http://elm.eu.org/; located in the N-terminal domain of Hdm2 in amino acids 26–101 of Hdm2) and is involved in the binding of p53 (called SWIB/Hdm2 domain). Given that residues 800–1,000 of UBE4B are required for the p53-UBE4B interaction, the SWIB/Hdm2 motif is located in residues 871–878 of UBE4B. We hypothesized that the SWIB/Hdm2 motif of UBE4B is essential for the p53-UBE4B interaction. We used the HPEPDOCK server to determine potential interaction between the SWIB/Hdm2 motif and p53 protein (HPEPDOCK, http://huanglab.phys.hust.edu.cn/hpepdock).[53,54] The HPEPDOCK server achieved a high success rate with predicted binding models compared with native structures.[53] The UBE4B peptide-p53 protein docking 3D models are shown in colors with the top ten predictions in Figure 5A, where the upper panel uses "cartoon"

(B) Western blot of UBE4B constructs, p53, and Hdm2 with FLAG-specific antibodies for UBE4B constructs, p53-specific (DO-1), and Myc-specific for Hdm2. (C) HCT116 stable clones expressing UBE4BΔ800–1,000, UBE4B, UBE4BΔU, or an empty vector were transiently transfected with a p21-Luc reporter plasmid, and luciferase activity was measured. Error bars indicate SEM (n = 3). $^{**}p < 0.01$; $^{***}p < 0.001$. (D) HCT116, $p53^{-/-}$ cells were transfected with p53 alone or p53 in combination with UBE4B, Hdm2, various UBE4B mutants, or an empty vector (pcDNA3) as indicated, and the cell-cycle profile was determined by propidium iodide staining and flow cytometry. The results represent the average of triplicate experiments. (E) HCT116, $p53^{-/-}$ cells were transfected with plasmids expressing p53 or p53 in combination with UBE4B, Hdm2, UBE4BΔ800–1,000, UBE4B 500–1,173, UBE4B 800–1,173, and UBE4B 1,000–1,100. The effect of various UBE4B constructs on p53-dependent apoptosis was determined by annexin V staining and flow cytometry. Error bars indicate SEM (n = 3). $^{*}p < 0.05$; $^{**}p < 0.01$; $^{***}p < 0.001$. (F) The levels of UBE4B mutants, p53, and Hdm2 expression were detected by western blotting. β-Actin was used as a loading control.

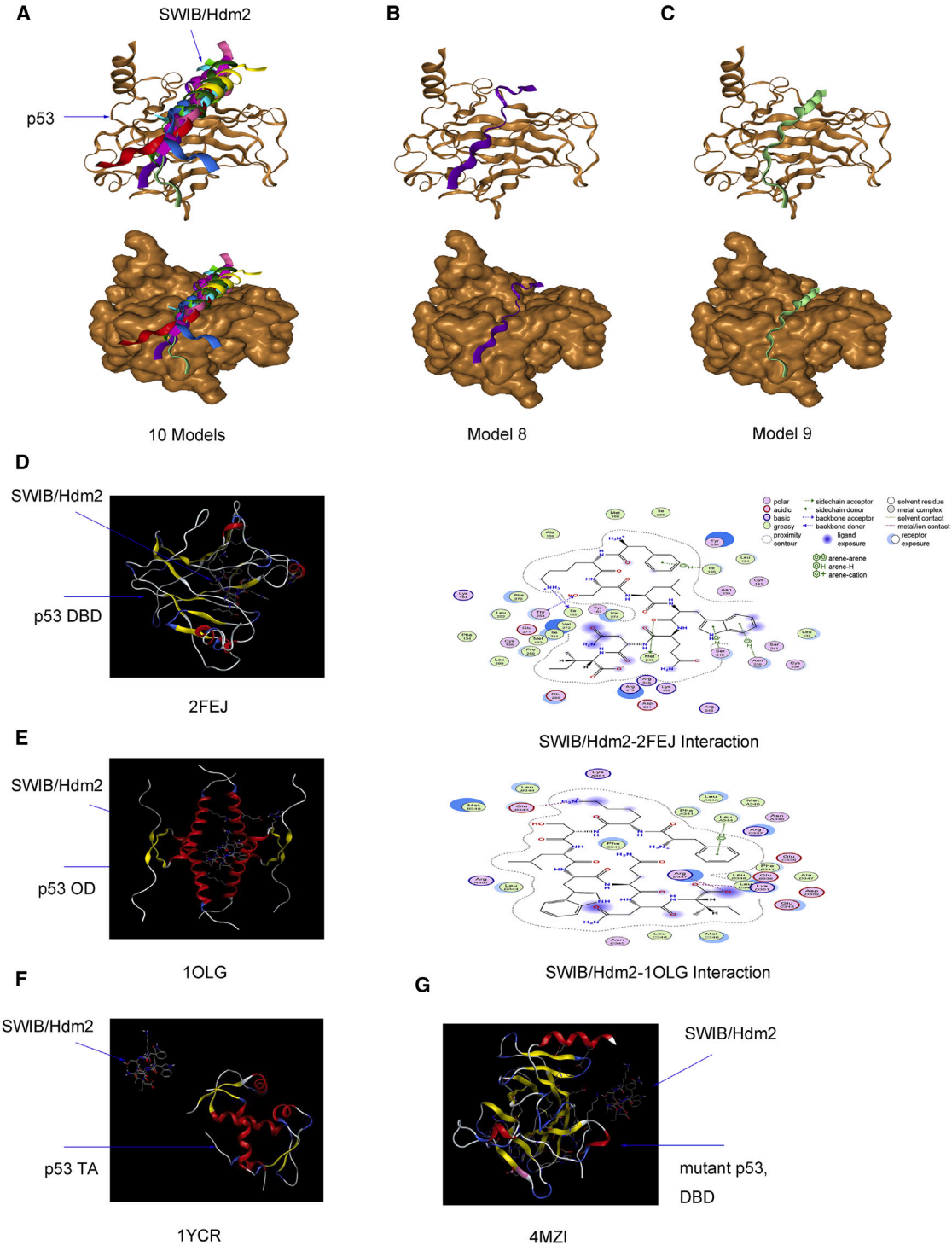

Figure 5. Peptide-protein molecular docking

(A) The location of the UBE4B peptide (top ten models with a different color) within the 3D structure of p53 DNA-binding domain (DBD) using HPEDOCK. In the upper panel we use the "cartoon" style for p53 protein and the SWIB/Hdm2 peptide; in the lower panel we use the molecular "surface" style for p53 protein and the "cartoon" style for the SWIB/Hdm2 peptide. (B) The location of a representative of the SWIB/Hdm2 peptide (model 8, purple) with the 3D structure of p53 DBD using HPEDOCK. (C) The location of a representative of the SWIB/Hdm2 peptide (model 9, green) with the 3D structure of p53 DBD using HPEDOCK. (D) The predicted binding model between the SWIB/Hdm2

(legend continued on next page)

style for the p53 protein and the UBE4B peptide and the lower panel uses molecular "surface" style for the p53 protein and "cartoon" style for the UBE4B peptide. Two locations of the UBE4B peptide within the 3D structure of the p53 protein from the HPEPDOCK web server with high docking scores are shown in Figures 5B and 5C, suggesting that there is a putative interaction between the SWIB/Hdm2 peptide and p53 protein. Similar data were obtained using several databases, including CABS-dock (http://biocomp.chem.uw.edu.pl/CABSdock) and Peptide2 (http://pepsite2.russelllab.org/). Molecular Operating Environment (MOE) software was used to determine the putative binding between the UBE4B peptide and p53 protein. As shown in Figures 5D–5F, we observed that the SWIB/Hdm2 motif of UBE4B forms a complex with the DNA-binding domain (DBD) (PDB: 2FEJ) and oligomerization domain (OD) of p53 (PDB: 1OLG), but the SWIB/Hdm2 motif does not bind to the transactivation domain of p53 (PDB: 1YCR). Interestingly, the SWIB/Hdm2 motif had no binding to a mutant p53 (PDB: 4MZI, Figure 5G). The 4MZI mutant contains seven single-point mutants, two-amino-acid mutants (SV changed to FG), and four-amino-acid mutants (HYNY changed to YFKF, www.rcsb.org). It is possible that the mutant p53 (PDB: 4MZI) might cause WT conformational changes. The predicted binding interactions of the UBE4B peptide (SWIB/Hdm2) with the binding sites of p53 (DBD and OD) are shown in Figures 5D and 5E (right panels). Together, these data suggested a potential interaction between the SWIB/Hdm2 motif and p53 (DBD and OD). We then analyzed the structure of UBE4B protein using two online programs (hanggroup.org/I-TASSER/ [University of Michigan][55–57] and https://open.predictprotein.org/). As predicted by the I-TASSER program, the SWIB/Hdm2 motif of UBE4B is probably exposed (Figure S1A). Possible ligand-binding residues are shown in blue stick representation in Figure S1B. Furthermore, we run "UCSF ChimeraX" software with the "AlphaFold" program,[58] and "https://colab.research.google.com/github/sokrypton/ColabFold/blob/main/AlphaFold2.ipynb#scrollTo=kOblAo-xetgx" online. The prediction 3D model of UBE4B by AlphaFold is shown in Figure S1C. Ufd2p core, SWIB/Hdm2 motif, and U box are color-labeled.

Inhibition of HCT116 cell growth by the SWIB/Hdm2 peptide

We then examined whether the SWIB/Hdm2 peptide derived from UBE4B binds to p53 *in vitro*. A series of p53 deletion mutants were expressed in *E. coli* as GST-tagged fusion proteins and purified (Figure 6A). A pull-down assay was performed to determine whether the SWIB/Hdm2 peptide interacts with p53. Consistently, the SWIB/Hdm2 peptide forms a stable complex with the DBD of p53 and has a weaker interaction with the C-terminal region of p53 (Figure 6B). In contrast, the control peptide did not pull down any truncations of p53 protein (Figure 6C). Given that peptide-protein interactions play a critical role in many cellular functions, we next investigated whether the SWIB/Hdm2 peptide inhibits UBE4B-mediated ubiquitination of p53. Notably, multiple ubiquitination of p53 mediated by UBE4B was significantly reduced with increasing amounts of the SWIB/Hdm2 peptide *in vitro* (Figure 6D). The formation of thioester bonds with Ub is a characteristic feature of the activity of E1 and E2.[59] To investigate whether the SWIB/Hdm2 peptide interferes with Ub transfer through the E1 (UBE1) or E2 (Ubch5b) cascade, a modified thioester assay was performed.[59] As shown in Figure 6E, Ub was able to form thioester conjugates with E1 without E2 and form Ub-E2 conjugates in the presence of E1. The SWIB/Hdm2 peptide did not block the formation of HA-Ub-E1 and HA-Ub-UbcH5b thioesters. As expected, HA-Ub-UbcH5b was not detected in the absence of E1 (Figure S1D). Furthermore, the SWIB/Hdm2 peptide does not affect UBE4B self-ubiquitination or activity (Figure S1E). Our findings indicated that the transfer of Ub to the E1 or E2 is not the target of the SWIB/Hdm2 peptide inhibition. To investigate whether the SWIB/Hdm2 peptide affects the UBE4B-p53 interaction, co-IP experiments were performed. HCT116 cells were treated with the control peptide or the SWIB/Hdm2 peptide (or so-called SWIB peptide), and immunoprecipitated with anti-p53 or anti-UBE4B antibodies as indicated. The ability of the SWIB/Hdm2 peptide to block the p53-UBE4B interaction was further demonstrated by co-IP (Figures 6F and 6G). Short peptides (5–30 amino acids) have a positive charge, which facilitates their penetration into cells throughout the cell membrane and nuclear membrane.[60] The biotin-labeled SWIB/Hdm2 peptide was detected by western blotting with an anti-biotin antibody using a vacuum-assisted detection method described previously (Figure S1F).[61,62] Next, we sought to determine whether the SWIB/Hdm2 peptide could affect p53-dependent cell growth. HCT116 cells were treated with the control peptide or the SWIB/Hdm2 peptide at indicated concentrations. Cell viability was determined by MTT cell viability assay.[63] Cell viability was significantly inhibited when the cells were treated with the SWIB/Hdm2 peptide compared with the cells treated with the control peptide (Figure 6H). Expression levels of p53 and UBE4B protein were measured by western blotting (Figures 6I and 6J). Importantly, cell viability did not show any change in HCT116, $p53^{-/-}$ cells treated with the SWIB/Hdm2 peptide or cells treated with the control peptide, indicating that this effect is mainly dependent on p53 (Figures 6K–6M).

The SWIB/Hdm2 motif activates p53

Next, we investigated whether the SWIB/Hdm2 peptide affects p53-dependent apoptosis. HCT116 cells were treated with the SWIB/Hdm2 peptide (20 μM) or control peptide. Annexin V staining was used to determine whether the cells treated with the SWIB/Hdm2 peptide could affect p53-dependent cell death. As shown in Figure 7A, HCT116 cells treated with the SWIB/Hdm2 peptide resulted in increased apoptosis compared with those treated with the control peptide. p53-Mediated cell-cycle arrest is crucial for its

motif and p53 DBD is shown in the left panel using MOE software (PDB: 2FEJ). The binding interaction of SWIB/Hdm2 with the binding site of p53 DBD is displayed in the right panel. (E) The predicted binding model between SWIB/Hdm2 motif and the p53 OD is shown in the left panel using MOE software (PDB: 1OLG). The binding interaction of SWIB/Hdm2 with the binding site of the p53 OD is displayed in the right panel. (F) The SWIB/Hdm2 motif does not bind to the transactivation domain of p53 using MOE software (PDB: 1YCR). (G) The SWIB/Hdm2 motif does not bind to mutant p53 using MOE software (PDB: 4MZI).

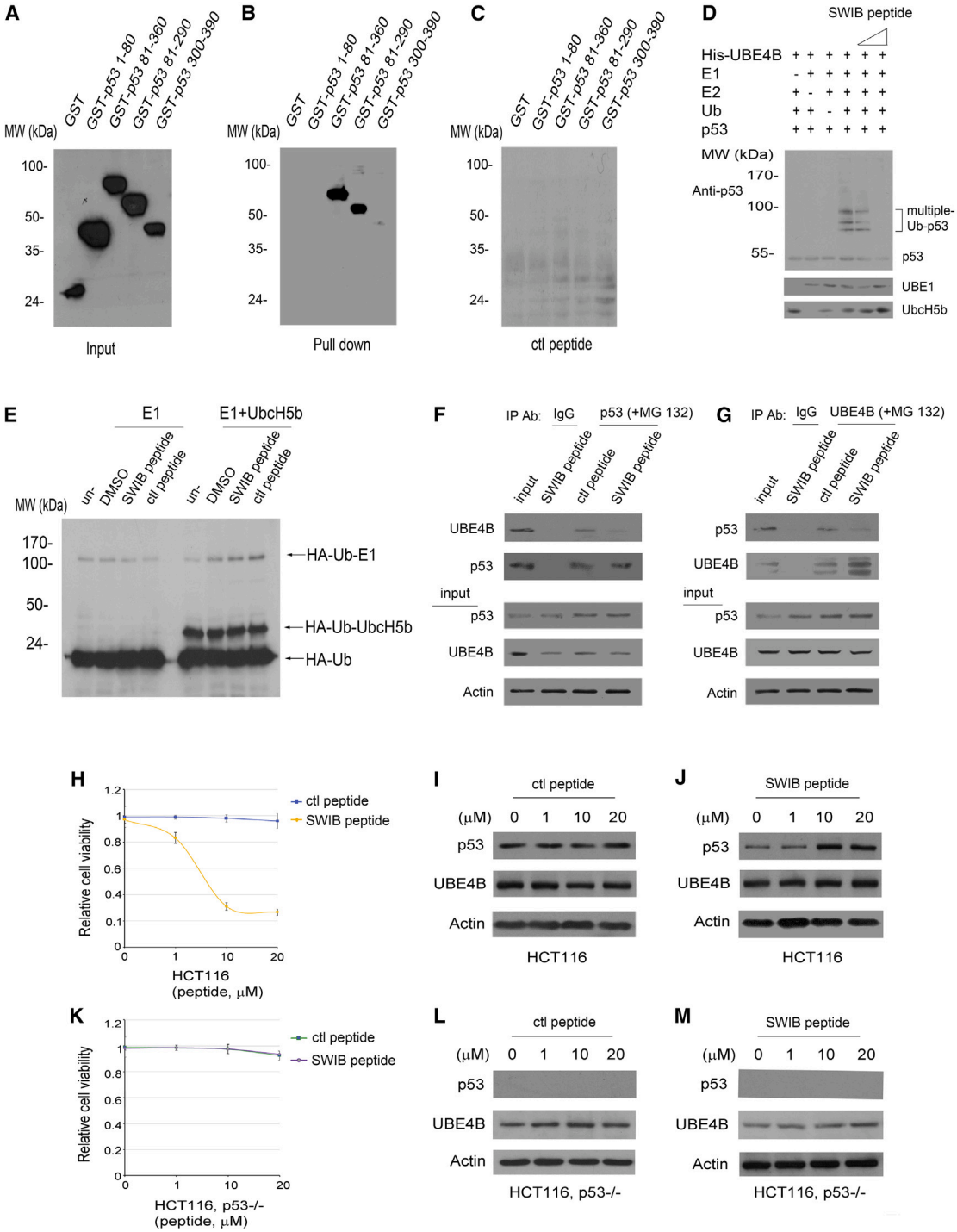

Figure 6. The SWIB/Hdm2 motif interacts with p53 and inhibits cell growth in WT p53 cancer cells

(A) GST-p53 fusion proteins were purified and analyzed by immunoblotting with a GST-specific antibody. (B) A biotinylated peptide pull-down assay was performed. Five microliters of biotinylated peptide (1.25 μg) was mixed with 2–4 μg of GST-p53 fusion proteins, and incubated at 4°C for 4 h. Streptavidin Sepharose beads were then added and incubated at 4°C for 1 h, washed, and analyzed by immunoblotting with an antibody against GST. (C) Similar to (B), except that the biotinylated control peptide was added. (D) His-UBE4B was evaluated for its E3 activity in the presence of recombinant E1, E2 (UbcH5b), Ub, p53, and the SWIB/Hdm2 peptide. Following the ubiquitination reaction, the samples were subjected to SDS-PAGE and immunoblotting with antibodies against p53 (DO-1) to reveal ubiquitinated p53, or E1 (UBE1) and E2 (UbcH5b) as indicated. (E) The SWIB/Hdm2 peptide does not block to form thioester conjugates with HA-Ub-E1 or HA-Ub-UbcH5b. The samples were subjected to nonreducing

(legend continued on next page)

tumor-suppression function. We tested whether the SWIB/Hdm2 peptide could affect p53-induced G_1 arrest.[34,41,40] As shown in Figure 7B, HCT116 cells treated with the SWIB/Hdm2 peptide exhibited an increase in the proportion of cells in G_1 phase and a decrease in the proportion of cells in S phase compared with the cells treated with the control peptide, resulting in an increase in the G_1/S ratio from 1.5 to 3.2. We then used a colony-formation assay for cell survival to monitor the long-term effects of the SWIB/Hdm2 peptide on p53 function. HCT116, $p53^{-/-}$ cells were transfected with plasmids expressing an empty vector, p53, or co-expression of p53 and UBE4B, or co-expression of p53 and UBE4BΔU. Cells were then treated with the SWIB/Hdm2 peptide or the control peptide, selected in G418 for 2 weeks, and the number of surviving colonies was counted. Expression of p53 dramatically inhibited colony formation compared with the cells treated with an empty vector. UBE4B effectively prevented p53-mediated cell death compared with the cells transfected with UBE4BΔU and treated with the control peptide (Figure 7C). Interestingly, the colony numbers were decreased in the cells with co-expression of p53 and UBE4B treated with the SWIB/Hdm2 peptide compared with the cells treated with the control peptide. In contrast, the colony numbers were further reduced by co-expression of p53 and UBE4BΔU compared with the cells co-expressing p53 and UBE4B treated with the SWIB/Hdm2 peptide, suggesting that the SWIB/Hdm2 peptide could largely block the interaction between p53 and UBE4B. Representative colony-formation assay results are presented in Figure 7D. Additionally, we used annexin V staining to determine whether the SWIB/Hdm2 peptide could affect p53-induced apoptosis by blocking the p53-UBE4B interaction. As expected, p53 expression alone resulted in increased apoptosis (Figure 7E). The increase in apoptosis could be prevented mainly by the co-expression of UBE4B but not UBE4BΔU when the cells were treated with the control peptide. Notably, p53-induced apoptosis largely prevented by co-expression of UBE4B could be significantly increased when the cells were treated with the SWIB/Hdm2 peptide. Next, we tested whether the SWIB/Hdm2 peptide affects p53-dependent cell-cycle arrest. A portion of the transfected HCT116, $p53^{-/-}$ cells treated with the SWIB/Hdm2 peptide or the control peptide was then subjected to cell-cycle analysis. We observed that p53-induced G_1 arrest could be significantly inhibited by co-expression of UBE4B treated with the control peptide, resulting in a decrease in the G_1/S ratio from 3.5 to 2.0, while the G_1/S ratio was increased from 2.0 to 3.1 when the cells were treated with the SWIB/Hdm2 peptide compared with the control peptide (Figure 7F). The levels of UBE4B, UBE4BΔU, p53, and p21 protein expression were verified by western blotting (Figure 7G). Taking the data together, the model we propose is shown in Figure 8. UBE4B, Hdm2, and p53 form a complex that promotes polyubiquitination and degradation of p53. The SWIB/Hdm2 motif derived from UBE4B binds and activates WT p53 functions by blocking the p53-UBE4B interaction.

DISCUSSION

The p53 tumor suppressor has been implicated in most human cancers. Therefore, a detailed understanding of the basis for its biological activation and regulation is a significant area of cancer research. The ability of Hdm2 to target p53 for degradation represents a key mechanism that controls the activity of p53 during cell growth. Our previous data revealed that UBE4B is required for Hdm2-mediated p53 polyubiquitination and degradation.[34] We then showed that UBE4B promotes degradation of phospho-p53 (S15 and S392), suggesting that UBE4B plays a role in regulating p53 after DNA damage.[64] In this study, we investigated the roles of different domains in UBE4B in the ubiquitination and degradation of p53. We found that the truncations of UBE4B affect its ability to target p53 for degradation. Notably, we identified one SWIB/Hdm2 motif of UBE4B and demonstrated that the SWIB/Hdm2 motif activates p53 by blocking the p53-UBE4B interaction.

As described previously, p53 and UBE4B interaction is necessary for p53 degradation.[34] We observed that UBE4BΔU (deleted U box) loses its ability to ubiquitinate and degrade p53. The UBE4BΔU mutant that fails to degrade p53 while retaining its ability to bind p53 is of particular interest because it acts in a dominant-negative manner. UBE4BΔU leads to stabilization of p53 but not UBE4B 1–1,000, although both fragments lack the C-terminal U-box domain. UBE4BΔU only deleted the U box (1,102–1,164 aa) and remained the longer C terminus of UBE4B. C-terminal Mdm2 mutants were reported to act as dominant negatives and increased p53 protein levels.[65] It is possible that adjacent sequences (around 1,001–1,101 aa of UBE4B) are required by UBE4B to function as a dominant negative to stabilize the p53 protein. This issue will have to be investigated in the future. Stabilization of endogenous p53 by the UBE4B mutant strongly supports previous studies that UBE4B is essential for the turnover of p53.

p53 is a known substrate of Hdm2 and UBE4B.[8–10,34–36] We previously showed that the interacting domains of UBE4B were mapped to the amino acids of the DBD and the C-terminal region in p53.[34] The binding site on UBE4B for p53 was assigned to the 800–1,000 aa regions of UBE4B. C-terminal UBE4B mutants lost their ability to degrade p53. We confirmed that UBE4BΔ800–1,000 failed to degrade p53 because the mutant could not bind to p53. The half-life of p53 was reduced to 10 min in the presence of UBE4B; on the

SDS-PAGE and analyzed by western blotting with an HA-specific antibody. (F) HCT116 cells were treated with 20 μM SWIB/Hdm2 peptide or control peptide for 40 h in the presence of 20 μM MG132, a proteasome inhibitor, as indicated, immunoprecipitated with a p53-specific antibody (Pab1801) or a control antibody (immunoglobulin G), and analyzed by western blotting with antibodies to detect UBE4B or p53. Western blots for p53, UBE4B, and actin are shown in the lower panels. (G) Similar to (F), except that an anti-UBE4B antibody was used. (H) HCT116 cells were treated with the control peptide or the SWIB/Hdm2 peptide at indicated concentrations for 40 h. Cell viability was examined by the MTT assay. (I) Western blot of HCT116 cells treated with different concentrations of the control peptide probed with antibodies against p53 (DO-1), UBE4B, and actin, as indicated. (J) Similar to (I), except that HCT116 cells were treated with the SWIB/Hdm2 peptide. (K) Similar to (H), except that HCT116, $p53^{-/-}$ cells were used. (L) Similar to (I), except that HCT116, $p53^{-/-}$ cells were used. (M) Similar to (J), except that HCT116, $p53^{-/-}$ cells were used.

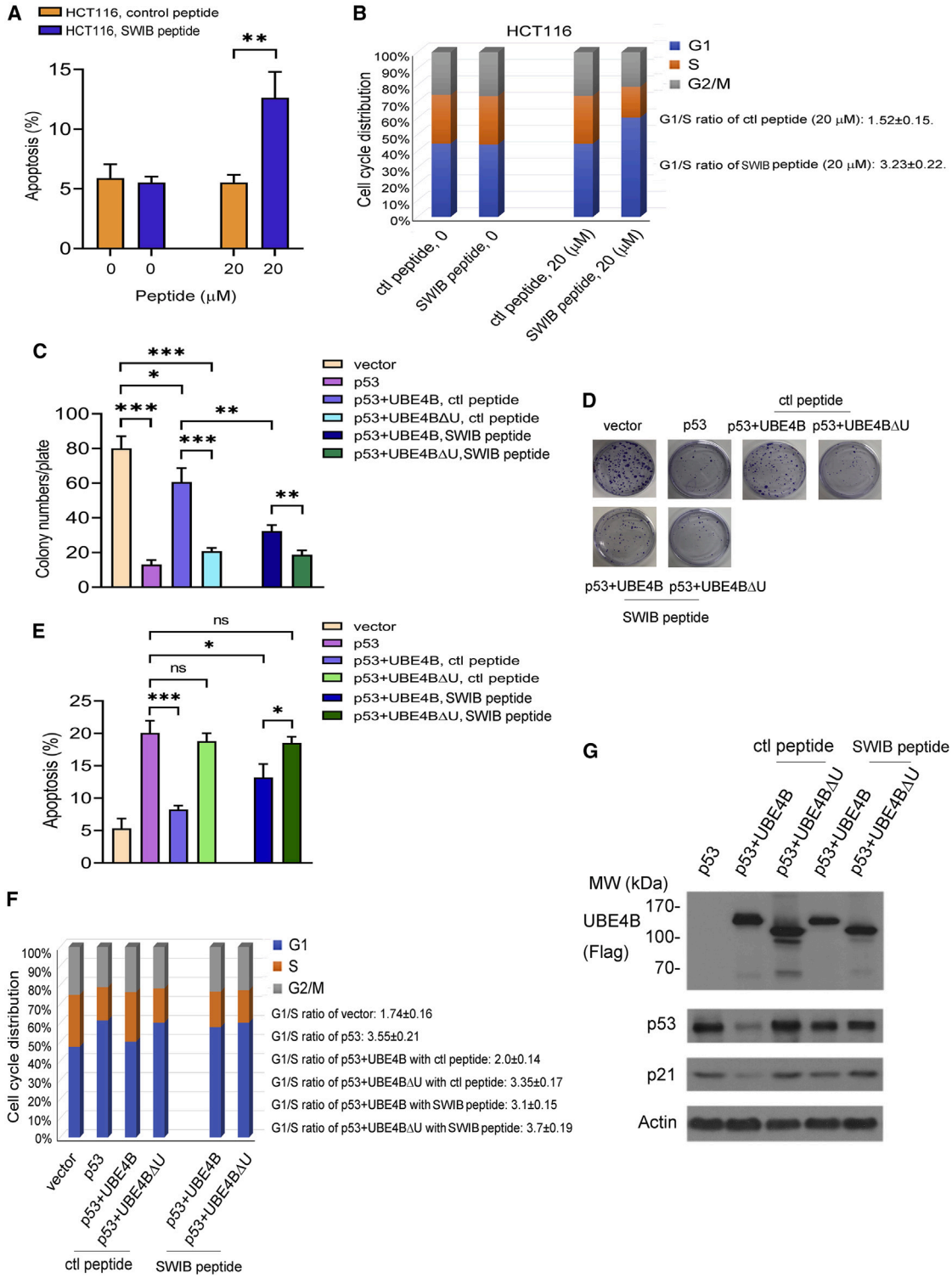

Figure 7. The SWIB/Hdm2 peptide activates p53

(A) HCT116 cells were treated with the control peptide or the SWIB/Hdm2 peptide (0 and 20 μM). The effect of the SWIB/Hdm2 peptide on p53-dependent apoptosis was determined by annexin V staining and flow cytometry. Error bars indicate SEM (n = 3). **p < 0.01. (B) HCT116 cells were treated with the control peptide or the SWIB/Hdm2 peptide as indicated. Propidium iodide staining and flow cytometry (left panel) were used to determine the cell-cycle profile. The results represent the average of three

(legend continued on next page)

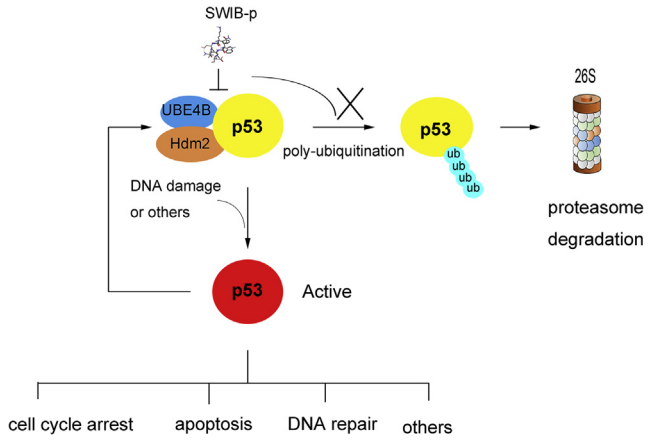

Figure 8. Model of p53 regulation and targeting the p53-UBE4B interaction
p53 is tightly regulated by Ub E3 ligases and is maintained at a low level under unstressed conditions. UBE4B, Hdm2, and p53 form a complex that promotes polyubiquitination and degradation of p53. The SWIB/Hdm2 motif derived from UBE4B was shown to bind to p53, reduce UBE4B-mediated ubiquitination of p53, and activate p53.

contrary, p53 has a half-life of approximately 40 min (UBE4BΔ800–1,000) and 80 min (UBE4BΔU), implying that the p53-UBE4B interaction and E3/E4 ligase activity of UBE4B are essential for the stability of p53. WT UBE4B promotes the ubiquitination of p53 in cells and *in vitro*. In contrast, UBE4BΔU was unable to promote p53 ubiquitination and degradation, indicating that ubiquitination activity is directly related to protein degradation. Furthermore, the C-terminal truncations of UBE4B and UBE4BΔ800–1,000 lost their ability for p53-dependent transactivation, cell-cycle arrest, and p53-dependent apoptosis.

Three residues—Phe19, Trp23, and Leu26—of p53 were identified as the key to its binding to Hdm2.[66] One SWIB-like domain was found in the N-terminal region of Hdm2 (26–101 aa). Several Hdm2-binding peptides based on p53 and Hdm2 inhibitors have entered clinical trials as an attractive strategy to restore WT p53 functions. Notably, we identified a putative SWIB/Hdm2 motif in UBE4B. Several docking software programs predict that the SWIB/Hdm2 motif interacts with p53 protein. Our results revealed that the SWIB/Hdm2 peptide binds directly to p53. Furthermore, the SWIB/Hdm2 peptide significantly inhibited the growth of HCT116 cells (harboring WT p53), but not in HCT116, $p53^{-/-}$ cells, implying that the growth inhibition of HCT116 cells by the SWIB/Hdm2 peptide is mainly dependent on p53. Flow-cytometric analysis using annexin V showed that the SWIB/Hdm2 peptide significantly induced apoptosis in HCT116 cells. p53 protein levels were decreased significantly when there was co-expression of UBE4B in the presence of the control peptide, while p53 protein levels did not change in cell co-expression of UBE4B treated with the SWIB/Hdm2 peptide, suggesting that the SWIB/Hdm2 peptide blocks the p53-UBE4B interaction.

An important question raised by our results based on the yeast Ufd2 protein structure and the AlphaFold model of UBE4B prediction is whether the SWIB/Hdm2 peptide is exposed or buried within the Ufd2p core domain. First, the structure of yeast Ufd2p (the only available Ufd2p structure) is different from human UBE4B for several reasons. (1) Yeast Ufd2p is encoded by a single copy gene;[24] on the contrary, two Ufd2-related genes have been found in *M. musculus* and *H. sapiens* (named UBE4A and UBE4B).[24–28] (2) Yeast Ufd2 is not essential for viability.[24,25] NOSA, the Ufd2 homolog of *D. discoideum*, is essential for cellular differentiation.[27] Deletion of Ube4b in mice results in embryonic lethality due to massive aopotosis.[29] (3) Yeast Ufd2 does not participate in the cascade of thioesters of the Ub enzyme and does not interact with the substrate directly.[26] In contrast, UBE4B functions as E3 (in the absence of other E3 components) to mediate ubiquitination of p53 in combination with E1 and E2 *in vitro*.[34] (4) In particular, no homolog of p53 is found in yeast. Second, AlphaFold is a useful tool but it cannot replace structure scientists. We further analyzed the structure of UBE4B protein using two online programs (hanggroup.org/I-TASSER/ [University of Michigan] and https://open.predictprotein.org/). Additionally, we ran "UCSF ChimeraX" software with the AlphaFold program. The SWIB/Hdm2 motif is likely exposed. Lastly, no SWIB/Hdm2 motif is found in yeast Ufd2p. The SWIB/Hdm2 motif is found in human UBE4B (http://elm.eu.org/). In addition, the SWIB/Mdm2 motif is found in mice Ube4b (http://elm.eu.org/). Therefore, it is exciting and important to study the structure of the p53-UBE4B complex by crystallography in the future.

In summary, our data revealed that 800–1,000 aa residues in UBE4B, and the U box of UBE4B, are essential for p53 degradation. Importantly, we discovered that the SWIB/Hdm2 peptide derived from UBE4B blocks the p53-UBE4B interaction and activates p53 functions, including p53-dependent transactivation and growth suppression. The newly identified SWIB/Hdm2 motif peptide may provide a new approach to cancer therapy in cancer patients with the somatic mutant p53.

MATERIALS AND METHODS

Cell culture and DNA transfection

HCT116 and HCT116, $p53^{-/-}$ isogenic human colon cancer cells were obtained from Dr. Bert Vogelstein (Johns Hopkins University,

experiments in triplicate. The G_1/S ratio is provided. (C) HCT116, $p53^{-/-}$ cells were transfected with plasmids expressing an empty vector, or p53, or combined with UBE4B or UBE4BΔU. At 30 h post transfection, cells were split, treated with the control peptide or the SWIB/Hdm2 peptide, and selected with G418, and colonies were stained after 2 weeks. The numbers were counted and plotted. All experiments were performed in triplicate. *$p < 0.05$; **$p < 0.01$; ***$p < 0.001$. (D) Representative colonies are shown as indicated. All experiments were performed in triplicate. (E) Similar to (A), except that HCT116, $p53^{-/-}$ cells were transfected with the indicated expression plasmids. Annexin V staining and flow cytometry were performed to detect cell apoptosis. *$p < 0.05$; ***$p < 0.001$. (F) Similar to (B), except that HCT116, $p53^{-/-}$ cells were transfected with the indicated expression plasmids. (G) Protein expression levels of UBE4B, UBE4BΔU, p53, and p21 were measured by western blotting. β-Actin was used as a loading control.

USA). These cell lines were cultured and frozen in liquid nitrogen immediately upon arrival and routinely tested by PCR for mycoplasma contamination using the following primers: Myco_fw1: 5′-ACA CCA TGG GAG CTG GTA AT-3′, Myco_rev1: 5′-CTT CAT CGA CTT TCA GAC CCA AGG CA-3′. HCT116 or HCT116, $p53^{-/-}$ cells were maintained in minimum essential medium (MEM) with 2 mM L-glutamine. MEM was adjusted to contain 1.5 g/L sodium bicarbonate, 0.1 mM nonessential amino acids, and 1.0 mM sodium pyruvate with 10% fetal bovine serum. For transient assays, expression plasmids were transfected into cells using calcium phosphate or Lipofectamine 2000 (Invitrogen). For stable clones of HCT116, cells were transfected with the indicated expression plasmids using Lipofectamine 2000 and selected in 500 μg/mL of Geneticin (G418) for 2 weeks.

Plasmids and antibodies

UBE4B or UBE4B mutants were amplified by PCR and cloned in pcDNA3.1 (Invitrogen) or p3x FLAG-CMV-10 (Sigma) or pET28a (Novagen). The Myc-Hdm2 expressing plasmid was a kind gift from Dr. A.G. Jochemsen. Hdm2 or Hdm2 mutants or p53 or p53 mutants were amplified by PCR and cloned into pcDNA3.1 or pET28a or pGEX5X1 (GE Healthcare). All PCR products were confirmed by sequencing. p53-Specific antibodies (Pab1801 and DO-1, Santa Cruz Biotechnology), Mdm2-specific antibodies (2A10, EMD Biosciences; SMP14, BD Biosciences), p21-specific antibody (F-5, Santa Cruz), Myc-specific antibody (9E10, Roche), FLAG-specific antibodies (M5 and M2, Sigma), Ub-specific antibody (P4D1, Santa Cruz), Ufd2/E4-specific antibodies (#611966, BD Biosciences), actin-specific antibody (A2228, Sigma), UBE1-specific antibody (Ab34711, Abcam), and UbcH5b-specific antibody (NBP1-81769, Novus Biologicals), and polyclonal antibodies for UBE4B (Ab97697, Abcam), anti-His (#70796-3, Novagen), anti-biotin (sc-101339), and anti-GST (B-14, Santa Cruz) were used according to the manufacturer's instructions.

Expression and preparation of recombinant protein

All GST or His-tagged recombinant proteins were expressed in *E. coli* strain BL21 (DE3, Novagene), treated with isopropyl-β-D-thiogalactoside to induce fusion protein expression, lysed by sonication, and purified using glutathione Sepharose 4B (GE Healthcare) for GST-fusion proteins or Ni2-NTA agarose (Qiagen) for His-fusion proteins.

Protein, peptide, molecular docking, and pull-down assays

The crystal structures and PDB files of human p53 were downloaded from the RCSB PDB database (www.rcsb.org). The structure and PDB file of the UBE4B peptide (also named SWIB/Hdm2 motif, FKSLWQNI) were generated by using Avogadro software (www.avogadro.cc) or MOE software, with a Site License to the University of Alberta, Chemical Computing Group Inc., Montreal, www.chemcomp.com). The HPEPDOCK (http://huanglab.phys.hust.edu.cn/hpepdock/), CABS-dock (http://biocomp.chem.uw.edu.pl/CABSdock), and Peptide2 (http://pepsite2.russelllab.org/) docking web servers were used to predict the possible interaction between the UBE4B motif (SWIB/Hdm2) and p53 protein. Molecular docking analysis was performed using MOE software (2022.08), including the removal of water molecules and co-crystallized molecules, energy minimization, docking stimulation, and ligand interactions. The predicted binding site(s) and interactions are shown. The UBE4B peptide (derived from the sequence of UBE4B; STIFKSLWQNIAHHG) and the control peptide (STIQWINFLSKAHHG) were synthesized (Invitrogen). Two biotinylated peptides were also synthesized. For the biotinylated peptide pull-down assay, 5 μL of biotinylated peptide (0.25 μg/μL) was added to purified GST-p53 fusion proteins (2–5 μg) and incubated at 4°C for 4 h. The mixtures were centrifuged for 15 min at 4°C to remove precipitating proteins, and the clarified lysates were mixed with streptavidin Sepharose beads previously washed with PBS and incubated for 1 h at 4°C with slow shaking. The bound beads were washed four times with the same buffer, heated at 95°C in SDS loading buffer, and analyzed by immunoblotting.

Immunoprecipitation and measurement of the half-life of p53

Cells were lysed in 50 mM Tris-HCl (pH 8.0), 1.0 mM EDTA, 150 mM NaCl, 0.5% NP-40, and protease inhibitor tablets (Roche), and immunoprecipitated with specific antibodies as indicated. The immune complexes were collected with protein A/G-Sepharose beads and washed four times with lysis buffer. The immunoprecipitants were analyzed by immunoblotting. To measure the half-life of p53, HCT116 cells were transfected with plasmids expressing WT UBE4B or UBE4B mutants or an empty vector. Twenty-four hours after transfection, cells were treated with 20 μg/mL cycloheximide (CHX) to inhibit *de novo* protein synthesis; protein levels were monitored by immunoblotting with anti-p53-specific antibodies at the indicated time points. The relative amount of p53 protein was determined by densitometry and normalized to β-actin.

In-cell ubiquitination assay

Cells were transfected with plasmids expressing p53, UBE4B, and various UBE4B constructs, either alone or in combination.[34,41,40] After 40 h, cells were harvested, lysed with RIPA buffer, and immunoprecipitated with the indicated antibodies. The immunoprecipitants recovered with protein A-Sepharose were washed four times with RIPA buffer (50 mM Tris-HCl [pH 7.6], 150 mM NaCl, 1.0% [v/v] NP-40, 0.5% [w/v] sodium deoxycholate, 1.0 mM EDTA, 0.5 mM EGTA, 1.0% [w/v] SDS, and protease inhibitor tablet [Roche]), separated on 10% SDS-PAGE, and analyzed by immunoblotting.

In vitro ubiquitination assay

As described previously, an *in vitro* ubiquitination assay with some modifications was performed.[34,41,40] For UBE4B mediated self-ubiquitination, rabbit E1 (20–40 ng, Calbiochem), UbcH5b (100 ng, Calbiochem), Ub (5 μg, Sigma), and His-UBE4B constructs (0.2–0.5 μg) were added to ubiquitination buffer (50 mM Tris-HCl [pH 7.4], 2.0 mM ATP, 5.0 mM MgCl, and 2.0 mM DTT) to a final volume of 20 μL. The reactions were incubated at 30°C for 1 h. The reactions were stopped with 2× SDS loading buffer, resolved by SDS-PAGE, and analyzed by western blotting. For UBE4B-mediated p53

ubiquitination, purified His-p53 protein was added as a substrate in the reaction described above.

Thioester assay

As described earlier, a thioester assay was performed with some modifications.[59,67] Reactions were added to E1 (100 ng, Calbiochem), HA-Ub (5 μg, Sigma), 20 μM control peptide or SWIB/Hdm2 peptide, or E1, UbcH5b (100 ng, Calbiochem), HA-Ub (5 μg, Sigma), 20 μM control peptide, or SWIB/Hdm2 peptide in reaction buffer (50 mM Tris-HCl [pH 7.4], 1 mM ATP, and 10 mM MgCl) to a final volume of 20 μL. The reactions were incubated for 1 h at room temperature. The reactions were stopped with 2× nonreducing SDS loading buffer, resolved by nonreducing SDS-PAGE gels, and analyzed by western blotting with an anti-HA antibody. To investigate whether the SWIB/Hdm2 peptide affects UBE4B autoubiquitination or activity, His-UBE4B and His-Ub were used for reaction in the presence of E1, E2. For nonreducing SDS-PAGE gel, there was no β-mercaptoethanol and DTT in the reaction.

MTT cell viability assay

As described previously,[63] HCT116 or HCT116, $p53^{-/-}$ cells were seeded at 5,000 cells/well in 96-well plates and treated with an increased amount of control peptide or the SWIB/Hdm2 peptide as indicated. After 40 h, 50 μL of MTT (3-(4,5-dimethylthiazol-2-yl)-2,5-diphenyl tetrazolium bromide) was added to each well and further incubated at 37°C for 4 h. The medium was washed with PBS and removed, and 150 μL of MTT solvent was added to each well. The absorbance was determined spectrophotometrically at 570 nm and normalized to the absorption value of the control well.

Western blots

Cells were harvested and lysed in 50 mM Tris-HCl (pH 8.0), 5.0 mM EDTA, 150 mM NaCl, 1% NP-40, and 1× protease inhibitor mixture (Roche). Proteins (20 or 40 μg of lysate) were resolved by SDS-PAGE. The proteins were transferred to Amersham Hybond-P membranes (GE Healthcare). The membranes were blocked in 5% (w/v) nonfat dried milk for 1 h and incubated with a primary antibody for 1 h at room temperature. The membranes were then washed and incubated with the appropriate horseradish peroxidase-conjugated secondary antibody (Jackson ImmunoResearch) for 1 h at room temperature. The proteins were detected by incubation with an ECL reagent (GE Healthcare). All band sizes were interpreted based on the migrations of standards with known molecular weights. We detected small peptides using 0.2-μm pore size PVDF, gradient of 4%–20%, and Tricine-SDS-PAGE by western blotting using a vacuum-assisted detection method.[61,62]

Luciferase assay

pGL3-E1bTATA contains a minimal promoter consisting of a TATA box downstream of one copy of the p53-binding site from the 5′ ends of the *p21WAF* promoter and is referred to as p21-Luc.[34,41] A galactosidase reporter construct, pCMV-gal (Promega), was included in all the transfection mixes. Luciferase activity was measured 2 days post transfection on samples containing equivalent amounts of protein using an LB9507 luminometer and the luciferase assay reagent (Promega); values were normalized to galactosidase activity.

Apoptosis assay

As described previously,[34,40,68] cells were transfected with the indicated expression plasmids for annexin V staining (BD Biosciences). The cells were then trypsinized, washed, and resuspended in PBS containing 25 μg/mL annexin-V-FITC and 50 μg/mL 7-aminoactinomycin D, and analyzed by flow cytometry.

Cell-cycle analysis

As previously described,[34,40,68] cells were transfected with the indicated expression plasmids. After 40 h the cells were washed, fixed with 70% ethanol, treated with 100 μg/mL RNase A, and labeled with 50 μg/mL propidium iodide for 3 h at 4°C and followed by flow cytometry (Becton Dickinson). Data were analyzed using FlowJo software (TreeStar).

Statistical analysis

Statistical significance was analyzed using a two-tailed Student's t test and expressed as a p value using GraphPad Prism 8 software. A p value of <0.05 was considered significant.

DATA AVAILABILITY

All other relevant data supporting the findings of this study are available within the article.

SUPPLEMENTAL INFORMATION

Supplemental information can be found online at https://doi.org/10.1016/j.omtn.2023.02.002.

ACKNOWLEDGMENTS

We thank Drs. M. Aminpour and J. Tuszynski (University of Alberta), who allowed us to use a Site License for the MOE software. We thank the University of Alberta for research equipment and technical support of this research. Initial funding from the Canadian Institutes of Health Research (CIHR) to R.L. started this research. A grant from the Natural Sciences and Engineering Research Council of Canada (NSERC) to R.L. supported this research. Y.A. was supported by a scholarship from Saudi Arabia. The graphical abstract was created using BioRender.com (granted a license "Academic License Terms," no. LB24R2ADYZ).

AUTHOR CONTRIBUTIONS

H.H.W., S.L., and Y.A. performed the experiments. H.H.W., S.L., and R.L. designed the study and analyzed the results. C.S. and D.D.E. provided support with the experimental techniques. H.H.W., S.L., and R.L. drafted the manuscript. C.S., D.D.E., and R.L. revised the manuscript. R.L. supervised the study. All authors read and approved the final manuscript.

DECLARATION OF INTERESTS

The authors declare no competing interests.

REFERENCES

1. Donehower, L.A., Harvey, M., Slagle, B.L., McArthur, M.J., Montgomery, C.A., Jr., Butel, J.S., and Bradley, A. (1992). Mice deficient for p53 are developmentally normal but susceptible to spontaneous tumours. Nature *356*, 215–221. https://doi.org/10.1038/356215a0.
2. Levine, A.J. (1997). p53, the cellular gatekeeper for growth and division. Cell *88*, 323–331. https://doi.org/10.1016/s0092-8674(00)81871-1.
3. Bieging, K.T., Mello, S.S., and Attardi, L.D. (2014). Unravelling mechanisms of p53-mediated tumour suppression. Nat. Rev. Cancer *14*, 359–370. https://doi.org/10.1038/nrc3711.
4. Sabapathy, K., and Lane, D.P. (2018). Therapeutic targeting of p53: all mutants are equal, but some mutants are more equal than others. Nat. Rev. Clin. Oncol. *15*, 13–30. https://doi.org/10.1038/nrclinonc.2017.151.
5. Levine, A.J. (2020). p53: 800 million years of evolution and 40 years of discovery. Nat. Rev. Cancer *20*, 471–480. https://doi.org/10.1038/s41568-020-0262-1.
6. Oliner, J.D., Pietenpol, J.A., Thiagalingam, S., Gyuris, J., Kinzler, K.W., and Vogelstein, B. (1993). Oncoprotein MDM2 conceals the activation domain of tumour suppressor p53. Nature *362*, 857–860. https://doi.org/10.1038/362857a0.
7. Leng, P., Brown, D.R., Shivakumar, C.V., Deb, S., and Deb, S.P. (1995). N-terminal 130 amino acids of MDM2 are sufficient to inhibit p53-mediated transcriptional activation. Oncogene *10*, 1275–1282.
8. Haupt, Y., Maya, R., Kazaz, A., and Oren, M. (1997). Mdm2 promotes the rapid degradation of p53. Nature *387*, 296–299. https://doi.org/10.1038/387296a0.
9. Kubbutat, M.H., Jones, S.N., and Vousden, K.H. (1997). Regulation of p53 stability by Mdm2. Nature *387*, 299–303. https://doi.org/10.1038/387299a0.
10. Honda, R., Tanaka, H., and Yasuda, H. (1997). Oncoprotein MDM2 is a ubiquitin ligase E3 for tumor suppressor p53. FEBS Lett. *420*, 25–27. https://doi.org/10.1016/s0014-5793(97)01480-4.
11. Roth, J., Dobbelstein, M., Freedman, D.A., Shenk, T., and Levine, A.J. (1998). Nucleo-cytoplasmic shuttling of the hdm2 oncoprotein regulates the levels of the p53 protein via a pathway used by the human immunodeficiency virus rev protein. EMBO J. *17*, 554–564. https://doi.org/10.1093/emboj/17.2.554.
12. Montes de Oca Luna, R., Wagner, D.S., and Lozano, G. (1995). Rescue of early embryonic lethality in mdm2-deficient mice by deletion of p53. Nature *378*, 203–206. https://doi.org/10.1038/378203a0.
13. Jones, S.N., Roe, A.E., Donehower, L.A., and Bradley, A. (1995). Rescue of embryonic lethality in Mdm2-deficient mice by absence of p53. Nature *378*, 206–208. https://doi.org/10.1038/378206a0.
14. Momand, J., Zambetti, G.P., Olson, D.C., George, D., and Levine, A.J. (1992). The mdm-2 oncogene product forms a complex with the p53 protein and inhibits p53-mediated transactivation. Cell *69*, 1237–1245. https://doi.org/10.1016/0092-8674(92)90644-r.
15. Wu, X., Bayle, J.H., Olson, D., and Levine, A.J. (1993). The p53-mdm-2 autoregulatory feedback loop. Genes Dev. *7*, 1126–1132. https://doi.org/10.1101/gad.7.7a.1126.
16. Kruse, J.P., and Gu, W. (2009). Modes of p53 regulation. Cell *137*, 609–622. https://doi.org/10.1016/j.cell.2009.04.050.
17. Piotrowski, J., Beal, R., Hoffman, L., Wilkinson, K.D., Cohen, R.E., and Pickart, C.M. (1997). Inhibition of the 26 S proteasome by polyubiquitin chains synthesized to have defined lengths. J. Biol. Chem. *272*, 23712–23721. https://doi.org/10.1074/jbc.272.38.23712.
18. Thrower, J.S., Hoffman, L., Rechsteiner, M., and Pickart, C.M. (2000). Recognition of the polyubiquitin proteolytic signal. EMBO J. *19*, 94–102. https://doi.org/10.1093/emboj/19.1.94.
19. Pickart, C.M. (2000). Ubiquitin in chains. Trends Biochem. Sci. *25*, 544–548. https://doi.org/10.1016/s0968-0004(00)01681-9.
20. Rodriguez, M.S., Desterro, J.M., Lain, S., Lane, D.P., and Hay, R.T. (2000). Multiple C-terminal lysine residues target p53 for ubiquitin-proteasome-mediated degradation. Mol. Cell Biol. *20*, 8458–8467. https://doi.org/10.1128/MCB.20.22.8458-8467.2000.
21. Lai, Z., Ferry, K.V., Diamond, M.A., Wee, K.E., Kim, Y.B., Ma, J., Yang, T., Benfield, P.A., Copeland, R.A., and Auger, K.R. (2001). Human mdm2 mediates multiple mono-ubiquitination of p53 by a mechanism requiring enzyme isomerization. J. Biol. Chem. *276*, 31357–31367. https://doi.org/10.1074/jbc.M011517200.
22. Grossman, S.R., Deato, M.E., Brignone, C., Chan, H.M., Kung, A.L., Tagami, H., Nakatani, Y., and Livingston, D.M. (2003). Polyubiquitination of p53 by a ubiquitin ligase activity of p300. Science *300*, 342–344. https://doi.org/10.1126/science.1080386.
23. Li, M., Brooks, C.L., Wu-Baer, F., Chen, D., Baer, R., and Gu, W. (2003). Mono- versus polyubiquitination: differential control of p53 fate by Mdm2. Science *302*, 1972–1975. https://doi.org/10.1126/science.1091362.
24. Johnson, E.S., Ma, P.C., Ota, I.M., and Varshavsky, A. (1995). A proteolytic pathway that recognizes ubiquitin as a degradation signal. J. Biol. Chem. *270*, 17442–17456. https://doi.org/10.1074/jbc.270.29.17442.
25. Hoppe, T., Matuschewski, K., Rape, M., Schlenker, S., Ulrich, H.D., and Jentsch, S. (2000). Activation of a membrane-bound transcription factor by regulated ubiquitin/proteasome-dependent processing. Cell *102*, 577–586. https://doi.org/10.1016/s0092-8674(00)00080-5.
26. Koegl, M., Hoppe, T., Schlenker, S., Ulrich, H.D., Mayer, T.U., and Jentsch, S. (1999). A novel ubiquitination factor, E4, is involved in multiubiquitin chain assembly. Cell *96*, 635–644. https://doi.org/10.1016/s0092-8674(00)80574-7.
27. Pukatzki, S., Tordilla, N., Franke, J., and Kessin, R.H. (1998). A novel component involved in ubiquitination is required for development of Dictyostelium discoideum. J. Biol. Chem. *273*, 24131–24138. https://doi.org/10.1074/jbc.273.37.24131.
28. Hoppe, T. (2005). Multiubiquitylation by E4 enzymes: 'one size' doesn't fit all. Trends Biochem. Sci. *30*, 183–187. https://doi.org/10.1016/j.tibs.2005.02.004.
29. Kaneko-Oshikawa, C., Nakagawa, T., Yamada, M., Yoshikawa, H., Matsumoto, M., Yada, M., Hatakeyama, S., Nakayama, K., and Nakayama, K.I. (2005). Mammalian E4 is required for cardiac development and maintenance of the nervous system. Mol. Cell Biol. *25*, 10953–10964. https://doi.org/10.1128/MCB.25.24.10953-10964.2005.
30. Matsumoto, M., Yada, M., Hatakeyama, S., Ishimoto, H., Tanimura, T., Tsuji, S., Kakizuka, A., Kitagawa, M., and Nakayama, K.I. (2004). Molecular clearance of ataxin-3 is regulated by a mammalian E4. EMBO J. *23*, 659–669. https://doi.org/10.1038/sj.emboj.7600081.
31. Okumura, F., Hatakeyama, S., Matsumoto, M., Kamura, T., and Nakayama, K.I. (2004). Functional regulation of FEZ1 by the U-box-type ubiquitin ligase E4B contributes to neuritogenesis. J. Biol. Chem. *279*, 53533–53543. https://doi.org/10.1074/jbc.M402916200.
32. Hosoda, M., Ozaki, T., Miyazaki, K., Hayashi, S., Furuya, K., Watanabe, K.I., Nakagawa, T., Hanamoto, T., Todo, S., and Nakagawara, A. (2005). UFD2a mediates the proteasomal turnover of p73 without promoting p73 ubiquitination. Oncogene *24*, 7156–7169. https://doi.org/10.1038/sj.onc.1208872.
33. Sirisaengtaksin, N., Gireud, M., Yan, Q., Kubota, Y., Meza, D., Waymire, J.C., Zage, P.E., and Bean, A.J. (2014). UBE4B protein couples ubiquitination and sorting machineries to enable epidermal growth factor receptor (EGFR) degradation. J. Biol. Chem. *289*, 3026–3039. https://doi.org/10.1074/jbc.M113.495671.
34. Wu, H., Pomeroy, S.L., Ferreira, M., Teider, N., Mariani, J., Nakayama, K.I., Hatakeyama, S., Tron, V.A., Saltibus, L.F., Spyracopoulos, L., and Leng, R.P. (2011). UBE4B promotes Hdm2-mediated degradation of the tumor suppressor p53. Nat. Med. *17*, 347–355. https://doi.org/10.1038/nm.2283.
35. Starita, L.M., Pruneda, J.N., Lo, R.S., Fowler, D.M., Kim, H.J., Hiatt, J.B., Shendure, J., Brzovic, P.S., Fields, S., and Klevit, R.E. (2013). Activity-enhancing mutations in an E3 ubiquitin ligase identified by high-throughput mutagenesis. Proc. Natl. Acad. Sci. USA *110*, E1263–E1272. https://doi.org/10.1073/pnas.1303309110.
36. Periz, G., Lu, J., Zhang, T., Kankel, M.W., Jablonski, A.M., Kalb, R., McCampbell, A., and Wang, J. (2015). Regulation of protein quality control by UBE4B and LSD1 through p53-mediated transcription. PLoS Biol. *13*, e1002114. https://doi.org/10.1371/journal.pbio.1002114.
37. Zhang, Y., Lv, Y., Zhang, Y., and Gao, H. (2014). Regulation of p53 level by UBE4B in breast cancer. PLoS One *9*, e90154. https://doi.org/10.1371/journal.pone.0090154.
38. Zhang, X.F., Pan, Q.Z., Pan, K., Weng, D.S., Wang, Q.J., Zhao, J.J., He, J., Liu, Q., Wang, D.D., Jiang, S.S., et al. (2016). Expression and prognostic role of ubiquitination factor E4B in primary hepatocellular carcinoma. Mol. Carcinog. *55*, 64–76. https://doi.org/10.1002/mc.22259.

39. Weng, C., Chen, Y., Wu, Y., Liu, X., Mao, H., Fang, X., Li, B., Wang, L., Guan, M., Liu, G., et al. (2019). Silencing UBE4B induces nasopharyngeal carcinoma apoptosis through the activation of caspase3 and p53. OncoTargets Ther. *12*, 2553–2561. https://doi.org/10.2147/OTT.S196132.

40. Wu, H.H., Wang, B., Armstrong, S.R., Abuetabh, Y., Leng, S., Roa, W.H.Y., Atfi, A., Marchese, A., Wilson, B., Sergi, C., et al. (2021). Hsp70 acts as a fine-switch that controls E3 ligase CHIP-mediated TAp63 and DeltaNp63 ubiquitination and degradation. Nucleic Acids Res. *49*, 2740–2758. https://doi.org/10.1093/nar/gkab081.

41. Leng, R.P., Lin, Y., Ma, W., Wu, H., Lemmers, B., Chung, S., Parant, J.M., Lozano, G., Hakem, R., and Benchimol, S. (2003). Pirh2, a p53-induced ubiquitin-protein ligase, promotes p53 degradation. Cell *112*, 779–791. https://doi.org/10.1016/s0092-8674(03)00193-4.

42. Böttger, V., Böttger, A., Howard, S.F., Picksley, S.M., Chène, P., Garcia-Echeverria, C., Hochkeppel, H.K., and Lane, D.P. (1996). Identification of novel mdm2 binding peptides by phage display. Oncogene *13*, 2141–2147.

43. Hietanen, S., Lain, S., Krausz, E., Blattner, C., and Lane, D.P. (2000). Activation of p53 in cervical carcinoma cells by small molecules. Proc. Natl. Acad. Sci. USA *97*, 8501–8506. https://doi.org/10.1073/pnas.97.15.8501.

44. Chipuk, J.E., Maurer, U., Green, D.R., and Schuler, M. (2003). Pharmacologic activation of p53 elicits Bax-dependent apoptosis in the absence of transcription. Cancer Cell *4*, 371–381. https://doi.org/10.1016/s1535-6108(03)00272-1.

45. Carvajal, D., Tovar, C., Yang, H., Vu, B.T., Heimbrook, D.C., and Vassilev, L.T. (2005). Activation of p53 by MDM2 antagonists can protect proliferating cells from mitotic inhibitors. Cancer Res. *65*, 1918–1924. https://doi.org/10.1158/0008-5472.CAN-04-3576.

46. Wagner, A.J., Banerji, U., Mahipal, A., Somaiah, N., Hirsch, H., Fancourt, C., Johnson-Levonas, A.O., Lam, R., Meister, A.K., Russo, G., et al. (2017). Phase I trial of the human double minute 2 inhibitor MK-8242 in patients with advanced solid tumors. J. Clin. Oncol. *35*, 1304–1311. https://doi.org/10.1200/JCO.2016.70.7117.

47. Carvajal, L.A., Neriah, D.B., Senecal, A., Benard, L., Thiruthuvanathan, V., Yatsenko, T., Narayanagari, S.R., Wheat, J.C., Todorova, T.I., Mitchell, K., et al. (2018). Dual inhibition of MDMX and MDM2 as a therapeutic strategy in leukemia. Sci. Transl. Med. *10*, eaao3003. https://doi.org/10.1126/scitranslmed.aao3003.

48. Konopleva, M., Martinelli, G., Daver, N., Papayannidis, C., Wei, A., Higgins, B., Ott, M., Mascarenhas, J., and Andreeff, M. (2020). MDM2 inhibition: an important step forward in cancer therapy. Leukemia *34*, 2858–2874. https://doi.org/10.1038/s41375-020-0949-z.

49. Gluck, W.L., Gounder, M.M., Frank, R., Eskens, F., Blay, J.Y., Cassier, P.A., Soria, J.C., Chawla, S., de Weger, V., Wagner, A.J., et al. (2020). Phase 1 study of the MDM2 inhibitor AMG 232 in patients with advanced P53 wild-type solid tumors or multiple myeloma. Invest. N. Drugs *38*, 831–843. https://doi.org/10.1007/s10637-019-00840-1.

50. Saleh, M.N., Patel, M.R., Bauer, T.M., Goel, S., Falchook, G.S., Shapiro, G.I., Chung, K.Y., Infante, J.R., Conry, R.M., Rabinowits, G., et al. (2021). Phase 1 trial of ALRN-6924, a dual inhibitor of MDMX and MDM2, in patients with solid tumors and lymphomas bearing wild-type TP53. Clin. Cancer Res. *27*, 5236–5247. https://doi.org/10.1158/1078-0432.CCR-21-0715.

51. Bennett-Lovsey, R., Hart, S.E., Shirai, H., and Mizuguchi, K. (2002). The SWIB and the MDM2 domains are homologous and share a common fold. Bioinformatics *18*, 626–630. https://doi.org/10.1093/bioinformatics/18.4.626.

52. Sczaniecka, M., Gladstone, K., Pettersson, S., McLaren, L., Huart, A.S., and Wallace, M. (2012). MDM2 protein-mediated ubiquitination of numb protein: identification of a second physiological substrate of MDM2 that employs a dual-site docking mechanism. J. Biol. Chem. *287*, 14052–14068. https://doi.org/10.1074/jbc.M111.303875.

53. Zhou, P., Jin, B., Li, H., and Huang, S.Y. (2018). HPEPDOCK: a web server for blind peptide-protein docking based on a hierarchical algorithm. Nucleic Acids Res. *46*, W443–W450. https://doi.org/10.1093/nar/gky357.

54. Yan, Y., Tao, H., He, J., and Huang, S.Y. (2020). The HDOCK server for integrated protein-protein docking. Nat. Protoc. *15*, 1829–1852. https://doi.org/10.1038/s41596-020-0312-x.

55. Yang, J., and Zhang, Y. (2015). I-TASSER server: new development for protein structure and function predictions. Nucleic Acids Res. *43*, W174–W181. https://doi.org/10.1093/nar/gkv342.

56. Zhang, C., Freddolino, P.L., and Zhang, Y. (2017). COFACTOR: improved protein function prediction by combining structure, sequence and protein-protein interaction information. Nucleic Acids Res. *45*, W291–W299. https://doi.org/10.1093/nar/gkx366.

57. Zheng, W., Zhang, C., Li, Y., Pearce, R., Bell, E.W., and Zhang, Y. (2021). Folding non- homology proteins by coupling deep-learning contact maps with I-TASSER assembly simulations. Cell Rep. Methods *1*, 100014. https://doi.org/10.1016/j.crmeth.2021.

58. Jumper, J., Evans, R., Pritzel, A., Green, T., Figurnov, M., Ronneberger, O., Tunyasuvunakool, K., Bates, R., Žídek, A., Potapenko, A., et al. (2021). Highly accurate protein structure prediction with AlphaFold. Nature *596*, 583–589. https://doi.org/10.1038/s41586-021- 03819-2.

59. Midgley, C.A., Desterro, J.M., Saville, M.K., Howard, S., Sparks, A., Hay, R.T., and Lane, D.P. (2000). An N-terminal p14ARF peptide blocks Mdm2-dependent ubiquitination in vitro and can activate p53 in vivo. Oncogene *19*, 2312–2323. https://doi.org/10.1038/sj.onc.1203593.

60. Khavinson, V.K., Popovich, I.G., Linkova, N.S., Mironova, E.S., and Ilina, A.R. (2021). Peptide regulation of gene expression: a systematic review. Molecules *26*, 7053. https://doi.org/10.3390/molecules26227053.

61. Schägger, H. (2006). Tricine-SDS-PAGE. Nat. Protoc. *1*, 16–22. https://doi.org/10.1038/nprot.2006.4.

62. Tomisawa, S., Abe, C., Kamiya, M., Kikukawa, T., Demura, M., Kawano, K., and Aizawa, T. (2013). A new approach to detect small peptides clearly and sensitively by Western blotting using a vacuum-assisted detection method. Biophysics *9*, 79–83. https://doi.org/10.2142/biophysics.9.79.

63. Chai, C., Wu, H., Wang, B., Eisenstat, D.D., and Leng, R.P. (2018). MicroRNA-498 promotes proliferation and migration by targeting the tumor suppressor PTEN in breast cancer cells. Carcinogenesis *39*, 1185–1196. https://doi.org/10.1093/carcin/bgy092.

64. Du, C., Wu, H., and Leng, R.P. (2016). UBE4B targets phosphorylated p53 at serines 15 and 392 for degradation. Oncotarget *7*, 2823–2836. https://doi.org/10.18632/oncotarget.6555.

65. Kubbutat, M.H., Ludwig, R.L., Levine, A.J., and Vousden, K.H. (1999). Analysis of the degradation function of Mdm2. Cell Growth Differ. *10*, 87–92.

66. Kussie, P.H., Gorina, S., Marechal, V., Elenbaas, B., Moreau, J., Levine, A.J., and Pavletich, N.P. (1996). Structure of the MDM2 oncoprotein bound to the p53 tumor suppressor transactivation domain. Science *274*, 948–953. https://doi.org/10.1126/science.274.5289.948.

67. Zhao, B., Bhuripanyo, K., Zhang, K., Kiyokawa, H., Schindelin, H., and Yin, J. (2012). Orthogonal ubiquitin transfer through engineered E1-E2 cascades for protein ubiquitination. Chem. Biol. *19*, 1265–1277. https://doi.org/10.1016/j.chembiol.2012.07.023.

68. Wang, B., Wu, H.H., Abuetabh, Y., Leng, S., Davidge, S.T., Flores, E.R., Eisenstat, D.D., and Leng, R. (2022). p63, a key regulator of Ago2, links to the microRNA-144 cluster. Cell Death Dis. *13*, 397. https://doi.org/10.1038/s41419-022-04854-1.